Site-Specific Bioconjugation

DOI: 10.1002/ange.201402613

Enzyme-Mediated Site-Specific Bioconjugation of Metal Complexes to Proteins: Sortase-Mediated Coupling of Copper-64 to a Single-Chain Antibody**

Brett M. Paterson, Karen Alt, Charmaine M. Jeffery, Roger I. Price, Shweta Jagdale, Sheena Rigby, Charlotte C. Williams, Karlheinz Peter, Christoph E. Hagemeyer, and Paul S. Donnelly**

Dedicated to Professor Jack M. Harrowfield on the occasion of his 70th birthday

Abstract: *The enzyme-mediated site-specific bioconjugation of a radioactive metal complex to a single-chain antibody using the transpeptidase sortase A is reported. Cage amine sarcophagine ligands that were designed to function as substrates for the sortase A mediated bioconjugation to antibodies were synthesized and enzymatically conjugated to a single-chain variable fragment. The antibody fragment $scFv_{anti\text{-}LIBS}$ targets ligand-induced binding sites (LIBS) on the glycoprotein receptor GPIIb/IIIa, which is present on activated platelets. The immunoconjugates were radiolabeled with the positron-emitting isotope ^{64}Cu. The new radiolabeled conjugates were shown to bind selectively to activated platelets. The diagnostic potential of the most promising conjugate was demonstrated in an in vivo model of carotid artery thrombosis using positron emission tomography. This approach gives homogeneous products through site-specific enzyme-mediated conjugation and should be broadly applicable to other metal complexes and proteins.*

The incorporation of selected radioactive isotopes into antibodies or antibody fragments combines the diagnostic and therapeutic possibilities of nuclear medicine with the exquisite selectivity of antibody targeting.[1] Engineered antibody derivatives, such as Fab fragments and single-chain variable fragments (scFv), aim to maintain specificity and selectivity with faster clearance from non-target tissue. A promising strategy to enable the use of metal radionuclides in antibody-targeted imaging and therapy is to design molecules that coordinate to the metal ion and preclude its release in vivo.[1a,2] The attachment of the chelator to the targeted antibody or fragment requires careful consideration to avoid compromising the affinity of the antigen-binding site for the target. Chelating ligands have traditionally been attached to antibodies through non-specific chemical conjugation reactions with the ε-amine of lysine residues or the thiol groups of cysteine residues. The multiple lysine and cysteine residues of monoclonal and scFv antibodies result in the formation of heterogeneous products with various numbers of chelators attached. Conjugations involving residues that are critical for antigen binding can compromise biological activity and are particularly problematic for antibody fragments because of their smaller size. Herein, we utilize an enzymatic site-specific conjugation strategy to attach metal complexes to an scFv antibody. The techniques and concepts presented are broadly applicable to a wide range of metal-ion chelators, antibodies, and antibody fragments.

Imaging technologies for the visualization of cellular and molecular processes in patients (molecular imaging) can assist clinicians in both diagnosis and monitoring treatment. Among the molecular imaging modalities, positron emission tomog-

[*] Dr. B. M. Paterson,[+] Assoc. Prof. P. S. Donnelly[+]
School of Chemistry and Bio21 Molecular Science and Biotechnology Institute, The University of Melbourne
Melbourne, Vic (Australia)
E-mail: pauld@unimelb.edu.au
Dr. K. Alt,[+] S. Jagdale, Dr. S. Rigby, Prof. K. Peter, Prof. C. E. Hagemeyer[+]
Vascular Biotechnology (K.A., C.E.H., S.J.), Atherothrombosis and Vascular Biology (K. A., K.P., S.R.)
Baker IDI Heart and Diabetes Institute
Melbourne, Vic (Australia)
E-mail: christoph.hagemeyer@bakeridi.edu.au
C. M. Jeffery, Prof. R. I. Price
Department of Medical Technology and Physics
Sir Charles Gairdner Hospital
Nedlands, WA (Australia)
Prof. R. I. Price
School of Physics, The University of Western Australia
Nedlands, WA (Australia)
Dr. C. C. Williams
CSIRO Materials Science and Engineering
343 Royal Parade, Melbourne, VIC (Australia)
Prof. K. Peter, Prof. C. E. Hagemeyer[+]
Central Clinical School, Monash University, Melbourne (Australia)
[+] These authors contributed equally to this work.

[**] This work was funded by the National Health and Medical Research Council (C.E.H, K.P.) and the Australian Research Council (P.S.D.). B.M.P. is supported by a Victorian Postdoctoral Research Fellowship funded by the Victorian Government. K.A. is supported by the German Research Foundation (Al 1521/1-1). K.P. and P.S.D. are Australian Research Council Future Fellows. C.E.H. is a National Heart Foundation Career Development Fellow. This research was undertaken using equipment provided by Monash Biomedical Imaging, Monash University as part of the Victorian Biomedical Imaging Capability (Victorian Government). Dr. Matt Harris (Clarity Pharmaceuticals) is thanked for his support.

Supporting information for this article is available on the WWW under http://dx.doi.org/10.1002/anie.201402613.

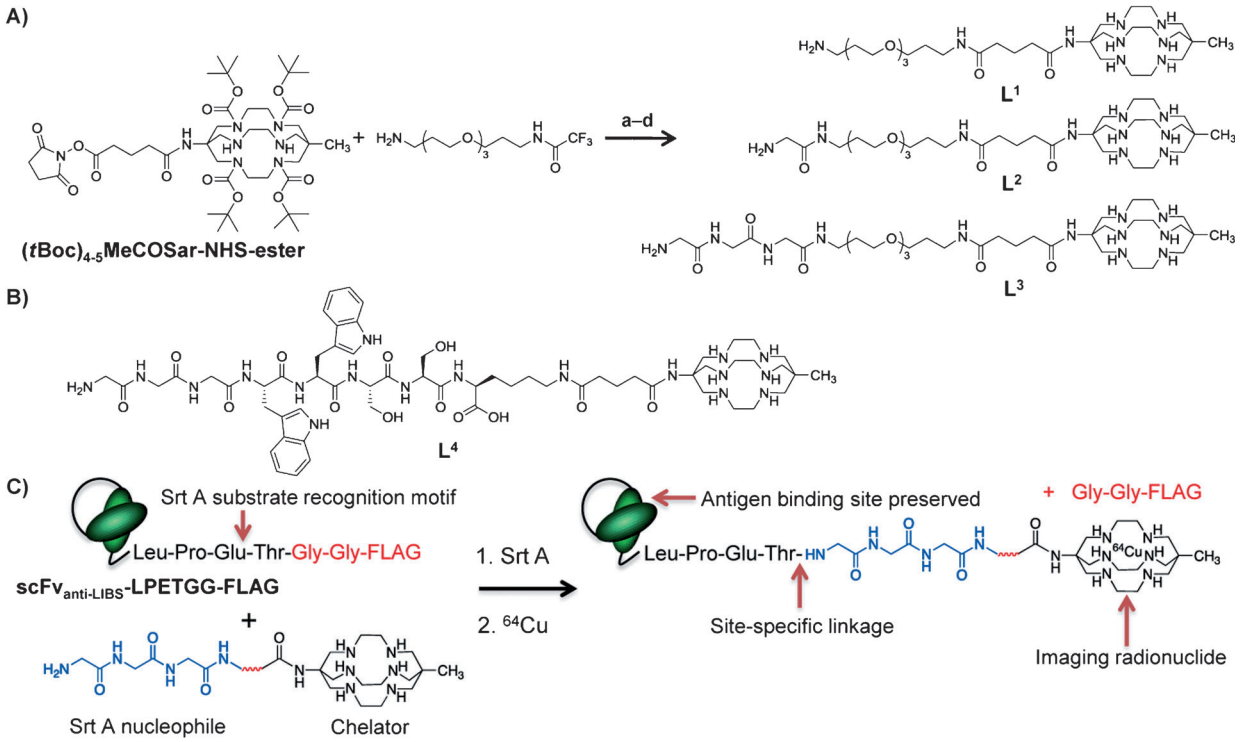

Figure 1. A) Synthesis of the sarcophagine (sar) bifunctional chelators $\mathbf{L^1}$–$\mathbf{L^3}$: a) methanol, RT, overnight; b) NaOH (1 M), pH > 11, RT, overnight; c) *t*Boc-Gly-OH ($\mathbf{L^2}$)/*t*Boc-Gly-Gly-Gly-OH ($\mathbf{L^3}$), HATU, DIPEA, DMF; d) trifluoroacetic acid. B) Structure of the peptide–sar bifunctional chelator $\mathbf{L^4}$. C) Sortase A (Srt A) mediated conjugation of the chelators to $scFv_{anti\text{-}LIBS}$–LPETGG–FLAG, followed by liberation and separation of the FLAG affinity tag and ^{64}Cu labelling of the products. DIPEA = *N*,*N*-diisopropylethylamine, DMF = *N*,*N*-dimethylformamide, HATU = *O*-(7-azabenzotriazol-1-yl)-*N*,*N*,*N*′,*N*′-tetramethyluronium hexafluorophosphate, *t*Boc = *tert*-butyloxycarbonyl.

raphy (PET) is becoming increasingly important to modern clinical practice. The radioisotope ^{64}Cu possesses attractive properties for PET imaging; the relatively low positron emission energy of 653 keV is similar to that of ^{18}F and results in high-quality images, and the half-life of 12.7 hours is suitable for agents with longer biological residence times. The ^{64}Cu radioisotope is best incorporated into a radiopharmaceutical by the formation of a thermodynamically stable and kinetically inert coordination complex.[3] Macrobicyclic cage amine ligands of the sarcophagine type (Figure 1) form very stable complexes with Cu^{2+} and are well suited for copper radioimmunoconjugates as radiolabeling can be achieved in high radiochemical yields at room temperature.[4]

Conjugation of radionuclides to antibodies includes modification of oligosaccharides attached to the Fc region and genetic engineering of proteins for direct chelation.[5] More recently, enzyme-mediated modifications have been utilized to radiolabel whole antibodies.[6] In contrast to conventional chemical conjugations, chemoenzymatic reactions are highly site-specific, robust, and reproducible and can be performed under mild conditions.

The transpeptidase sortase A (Srt A) is produced by Gram-positive bacteria and covalently attaches cell surface proteins to the cell wall.[7] In bacteria, Srt A cleaves an amide bond between Thr and Gly in the small pentapeptide recognition motif Leu-Pro-*X*-Thr-Gly (where *X* = any amino acid).[8] The Leu-Pro-*X*-Thr-Gly "sorting tag" can be included in recombinantly expressed proteins or antibodies to allow site-specific enzyme-mediated bioconjugation. The structure and function of antibodies is not compromised by the presence of the small sorting tag, and loss of biological activity is rarely observed.[8f,9]

The single-chain variable fragment $scFv_{anti\text{-}LIBS}$, which targets the ligand-induced binding sites (LIBS) on the glycoprotein receptor GPIIb/IIIa, has potential to be used as a targeting agent for the diagnosis of thrombosis and inflammation.[10] The $scFv_{anti\text{-}LIBS}$ agent is selective for activated platelets over circulating platelets, which is an advantage when compared to anti-GPIIb/IIIa antibodies or peptides, which also bind to non-activated platelets.[11] Furthermore, in contrast to $scFv_{anti-LIBS}$, RGD peptides can induce platelet activation and may therefore be unsuitable for diagnostic imaging in patients.[12] We have previously demonstrated that indiscriminate chemical conjugation of small-molecule radiopharmaceuticals to the lysine residues of $scFv_{anti\text{-}LIBS}$ resulted in some impairment of antigen binding.[13]

Herein, we describe the synthesis of new sarcophagine derivatives designed to function as substrates for Srt A and demonstrate their conjugation to $scFv_{anti\text{-}LIBS}$, which is catalyzed by Srt A. One of the first challenges was that affinity chromatography with the use of a $scFv_{anti-LIBS}$ cloned with a His6 affinity tag after the LPETGG motif (which is conveniently cleaved during the enzymatic conjugation)[9a,c] was not possible as the sarcophagine chelator strips the Ni^{2+} from the purification column. This problem was circumvented by the use of a variant with a FLAG

affinity tag at the C terminus of $scFv_{anti-LIBS}$ and the Srt A enzyme.[14]

To enable site-specific conjugation to $scFv_{anti-LIBS}$–LPETGG–FLAG using Srt A, the bifunctional chelator MeCOSar[15] (Figure 1 A) was elaborated with glycine-containing short-chain oligo(ethylene glycol) (OEG) linkers.[16] The scope and tolerance of the Srt A mediated enzymatic reaction was investigated with the chelator MeCOSar with four different peptide functional groups. The first step in the synthesis of $\mathbf{L^1}$–$\mathbf{L^3}$ was the protection of a single amine of 4,7,10-trioxatridecane-1,13-diamine by reaction with ethyltrifluoroacetate. In the next step, this amine was added to the *N*-hydroxysuccinimide activated $(t\text{Boc})_{4\text{-}5}$MeCOSar-NHS ester, which was followed by the removal of the trifluoroacetamide group. (Figure 1 A). The bifunctional chelators $\mathbf{L^1}$ (no Gly residue), $\mathbf{L^2}$ (one Gly residue), and $\mathbf{L^3}$ (three Gly residues) were characterized by NMR spectroscopy and ESI mass spectrometry. The ^{13}C NMR spectra, which were acquired in D_2O, indicated the presence of the glycine CH_2 groups for both $\mathbf{L^2}$ ($\delta = 41.0$ ppm) and $\mathbf{L^3}$ ($\delta = 41.1$, 43.0, and 43.2 ppm). Aside from the aminoglycine short-chain OEG linkers, a triglycine-containing peptide (GGGWWSSK), which has been shown to be an efficient Srt A substrate,[9a] was also attached to MECOSar through the ε-amino group of the C-terminal lysine residue using solid-phase peptide synthesis and 9-fluorenylmethyloxycarbonyl (Fmoc) and (4-methoxyphenyl)(diphenyl)methyl (Mmt) protecting groups to give $\mathbf{L^4}$ (Figure 1 B).

Each bifunctional chelator was allowed to react with $scFv_{anti-LIBS}$–LPETGG–FLAG in the presence of Srt A for five hours at 37 °C (Figure 1 C). The products were purified by anti-FLAG affinity chromatography, and their identity and purity were confirmed with SDS-PAGE page and ESI mass spectrometry (SDS-PAGE = sodium dodecylsulfate–polyacrylamide gel electrophoresis; Figure 2). The reaction with $\mathbf{L^1}$ resulted in a poor yield (ca. 30 %). The best yields were obtained using $\mathbf{L^2}$ and $\mathbf{L^4}$ (ca. 90 %). The construct from $\mathbf{L^3}$ was obtained in poor yield (ca. 50 %) despite the presence of three Gly residues.

The sortase-mediated coupling is reversible because the products $\mathbf{L^2}$–$\mathbf{L^4}$ contain LPETG sequences. It is possible that the good yield of $scFv_{anti-LIBS}$–LPET–$\mathbf{L^2}$ is due to the presence of the OEG linker directly next to the single glycine residue, which impairs the reverse reaction. The product $scFv_{anti-LIBS}$–LPET–$\mathbf{L^4}$ was generated in good yield because of the presence of Trp residues (LPETGGGWW), which slows the rate of the reverse reaction, presumably because of the steric bulk of the indole side chain.[17] The deconvoluted ESI mass spectra of $scFv_{anti-LIBS}$–LPET–$\mathbf{L^2}$ and $scFv_{anti-LIBS}$–LPET–$\mathbf{L^4}$ are shown in Figure 2, with the mass-to-charge (m/z) distributions centered at 31 064 Da and 31 650 Da, respectively ($\mathbf{L^2}$: 687 g mol^{-1}; $\mathbf{L^4}$: 1273 g mol^{-1}). The selectivity of the immunoconjugates for platelets that were activated by the addition of adenosine diphosphate (20 μM) was assessed using fluorescence-activated cell sorting (FACS), which indicated strong binding to the target (Figure 2; see also the Supporting Information). None of the constructs bound to non-activated platelets. Both $\mathbf{L^2}$ and $\mathbf{L^4}$ gave good yields in Srt A mediated reactions; however, as $\mathbf{L^2}$ is easier to synthesize and has

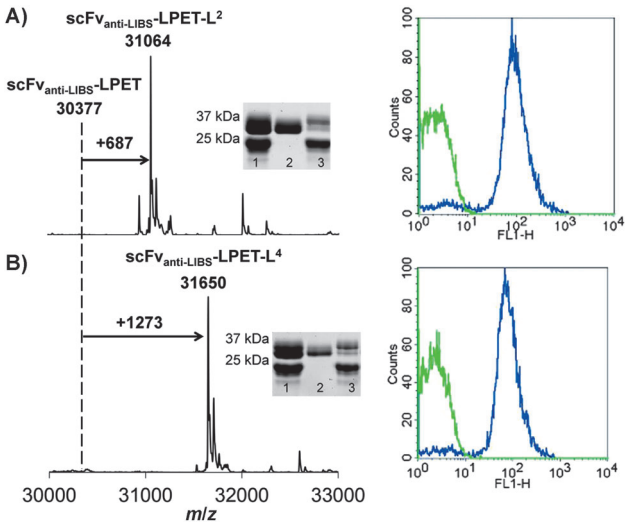

Figure 2. A, B) ESI mass spectra of $scFv_{anti-LIBS}$–LPET–$\mathbf{L^2}$ (A) and $scFv_{anti-LIBS}$–LPET–$\mathbf{L^4}$ (B). Insets: SDS-PAGE analysis of 1) the non-purified reaction mixture; 2) purified $scFv_{anti-LIBS}$–LPET–$\mathbf{L^2}$ (A) and $scFv_{anti-LIBS}$–LPET–$\mathbf{L^4}$ (B); and 3) Srt A ($M_W = 17.9$ kDa) and $scFv_{anti-LIBS}$–LPETGG–FLAG ($M_W = 33.5$ kDa) after elution from the anti-FLAG affinity chromatography column. Right-hand side: FACS histograms showing the binding of $scFv_{anti-LIBS}$–LPET–$\mathbf{L^2}$ (A) and $scFv_{anti-LIBS}$–LPET–$\mathbf{L^4}$ (B) to activated platelets (blue line) and non-activated platelets (green line).

a lower molecular weight, it was used for further studies. Aside from $scFv_{anti-LIBS}$–LPET–$\mathbf{L^2}$, a mutant variant ($scFv_{mut}$–LPET–$\mathbf{L^2}$) was synthesized using Srt A mediated conjugation and used as a control for determining the degree of antigen specificity. The mutant variant is based on an Arg-Gly-Asp (RGD) mutation of the parent antibody resulting in complete loss of binding to GPIIb/IIIa.[18]

The immunoconjugates were radiolabeled with $^{64}Cu^{2+}$ at pH 7 and room temperature in less than 30 minutes with a radiochemical purity of > 95 %. The antigen binding of the conjugate with $^{64}Cu^{2+}$ coordinated to the chelator was comparable to that of copper-free $scFv_{anti-LIBS}$–LPET–$\mathbf{L^2}$ and the unmodified $scFv_{anti-LIBS}$, and neither construct bound to non-activated platelets (data not shown).

The targeting abilities of the immunoconjugates $scFv_{anti-LIBS}$–LPET–$^{64}Cu\mathbf{L^2}$ and $scFv_{mut}$–LPET–$^{64}Cu\mathbf{L^2}$, which were radiolabeled with ^{64}Cu, towards activated platelets were evaluated in an in vivo model of mouse carotid artery thrombosis, which was induced by exposure to $FeCl_3$.[9c,10a,c,13,19] The biodistribution data confirmed a significant increase in $scFv_{anti-LIBS}$–LPET–$^{64}Cu\mathbf{L^2}$ uptake in the injured vessel (34.01 ± 7.9 % ID/g) compared to the non-injured vessel (14.25 ± 5.5 % ID/g, $p = 0.0001$) and the muscle as control (0.59 ± 0.36 % ID/g, $p = 0.0001$; Figure 3). In the injured vessel, the uptake of $scFv_{anti-LIBS}$–LPET–$^{64}Cu\mathbf{L^2}$ was significantly higher than that of $scFv_{mut}$–LPET–$^{64}Cu\mathbf{L^2}$ (13.03 ± 11.48 % ID/g, $p = 0.0001$). In a separate study, administration of $scFv_{anti-LIBS}$ (400 μg) 30 minutes before radiotracer injection to block the binding sites significantly reduced the binding of $scFv_{anti-LIBS}$–LPET–$^{64}Cu\mathbf{L^2}$ to the target receptor ($p = 0.0001$; Figure 3). The mice were placed in a small-animal PET/CT scanner (CT = computed tomogra-

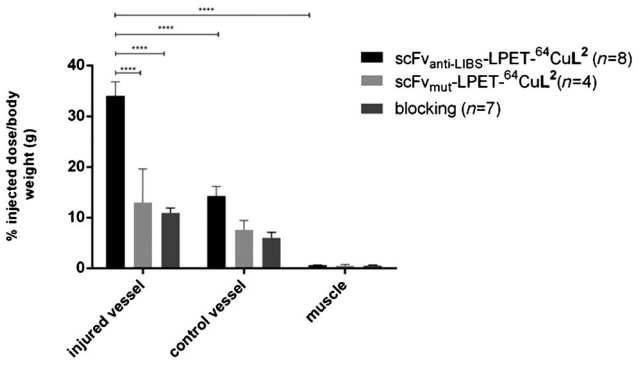

Figure 3. Biodistribution of scFv$_{anti-LIBS}$–LPET–^{64}Cu**L**^{2} (black) and scFv$_{mut}$–^{64}Cu**L**^{2} (light grey) in the injured vessel compared to the non-injured vessel and the muscle. Blocking of scFv$_{anti-LIBS}$–LPET–^{64}Cu**L**^{2} uptake (dark grey) in an in vivo model of mouse carotid artery thrombosis with 400 μg of non-radioactive scFv$_{anti-LIBS}$, which was administered 30 minutes before radiotracer injection. Data are given as the percentage of the injected dose per body weight (g) and were measured 90 minutes after tracer injection (****/$p = 0.0001$).

phy) 30 minutes after injection of a single dose of scFv$_{anti-LIBS}$–LPET–^{64}Cu**L**^{2} or scFv$_{mut}$–LPET–^{64}Cu**L**^{2} (3–5 MBq) with the carotid artery set as the region of interest. The PET/CT scans showed an accumulation of scFv$_{anti-LIBS}$–LPET–^{64}Cu**L**^{2} in the injured vessel and no significant uptake of scFv$_{mut}$–LPET–^{64}Cu**L**^{2}, which confirms that GPIIb/IIIa mediated binding is highly specific (Figure 4).

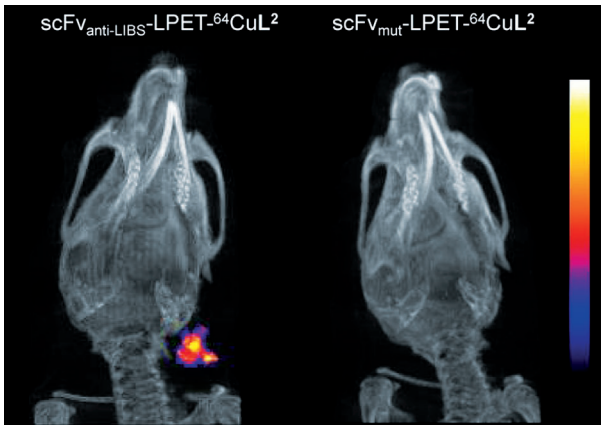

Figure 4. Serial small-animal PET/CT images of an in vivo model of mouse carotid artery thrombosis. Comparison of representative maximum-intensity projection PET images of scFv$_{anti-LIBS}$–LPET–^{64}Cu**L**^{2} and scFv$_{mut}$–^{64}Cu**L**^{2} 60 minutes after injection of the radiotracer. The color scale for all PET image data shows radiotracer uptake with white and blue corresponding to the highest and lowest activity, respectively.

In summary, we have reported the synthesis and isolation of bifunctional chelators and demonstrated their ability for high-yielding, site-specific, and reproducible modification of an scFv antibody against the platelet integrin GPIIb/IIIa in its active ligand-bound form using Srt A. Sortase-mediated bioconjugation is particularly beneficial for modifying antibody fragments that lack the readily accessible and modifiable oligosaccharide side chains of full antibodies. The high level of specific binding to activated platelets was maintained upon enzyme-mediated conjugation and radiolabelling of the immunoconjugate products and suggests that they have the potential to be of use for the in vivo detection of activated platelets for early diagnosis of acute thrombotic events, such as myocardial infarction and ischemic stroke, as well as inflammation. Advances in antibody development have resulted in rapid growth in this area of human therapeutics and a dramatically increasing number of FDA-approved agents. Much of the experience gained from the generation and optimization of one antibody is applicable to other antibodies. The specificity and selectivity of antibodies can be exploited for PET imaging and targeted radiotherapy but the construction of radionuclide–antibody agents requires careful consideration to maximize biological efficacy. The approach described here gives rise to homogeneous products through site-specific and controlled enzyme-mediated conjugation and should be broadly applicable to other metal complexes and proteins.

Received: February 20, 2014
Published online: April 28, 2014

Keywords: bioconjugation · bioinorganic chemistry · copper · macrocyclic ligands · radiopharmaceuticals

[1] a) C. F. Meares, *Nucl. Med. Biol.* **1986**, *13*, 311; b) C. A. Boswell, M. W. Brechbiel, *Nucl. Med. Biol.* **2007**, *34*, 757.
[2] E. W. Price, C. Orvig, *Chem. Soc. Rev.* **2014**, *43*, 260.
[3] T. J. Wadas, E. H. Wong, G. R. Weisman, C. J. Anderson, *Chem. Rev.* **2010**, *110*, 2858.
[4] a) A. M. Sargeson, *Coord. Chem. Rev.* **1996**, *151*, 89; b) S. D. Voss, S. V. Smith, N. Di Bartolo, L. J. McIntosh, E. M. Cyr, A. A. Bonab, J. L. J. Dearling, E. A. Carter, A. J. Fischman, S. T. Treves, S. D. Gillies, A. M. Sargeson, J. S. Huston, A. B. Packard, *Proc. Natl. Acad. Sci. USA* **2007**, *104*, 17489; c) M. S. Cooper, M. T. Ma, K. Sunassee, K. P. Shaw, J. D. Williams, R. L. Paul, P. S. Donnelly, P. J. Blower, *Bioconjugate Chem.* **2012**, *23*, 1029; d) H. Cai, Z. Li, C.-W. Huang, R. Park, A. H. Shahinian, P. S. Conti, *Nucl. Med. Biol.* **2010**, *37*, 57.
[5] a) J. D. Rodwell, V. L. Alvarez, C. Lee, A. D. Lopes, J. W. F. Goers, H. D. King, H. J. Powsner, T. J. McKearn, *Proc. Natl. Acad. Sci. USA* **1986**, *83*, 2632; b) J. T. Tait, C. Smith, Z. Levashova, B. Patel, F. G. Blankenberg, J.-L. Vanderheyden, *J. Nucl. Med.* **2006**, *47*, 1546; c) M. V. Backer, Z. Levashova, V. Patel, B. T. Jehning, K. Claffey, F. G. Blankenberg, J. M. Backer, *Nat. Med.* **2007**, *13*, 504.
[6] a) S. Jeger, K. Zimmermann, A. Blanc, J. Gruenberg, M. Honer, P. Hunziker, H. Struthers, R. Schibli, *Angew. Chem.* **2010**, *122*, 10191; *Angew. Chem. Int. Ed.* **2010**, *49*, 9995; b) B. M. Zeglis, C. B. Davis, R. Aggeler, H. C. Kang, A. Chen, B. J. Agnew, J. S. Lewis, *Bioconjugate Chem.* **2013**, *24*, 1057.
[7] S. K. Mazmanian, G. Liu, H. Ton-That, O. Schneewind, *Science* **1999**, *285*, 760.
[8] a) H. Ton-That, G. Liu, S. K. Mazmanian, K. F. Faull, O. Schneewind, *Proc. Natl. Acad. Sci. USA* **1999**, *96*, 12424; b) X. Huang, A. Aulabaugh, W. Ding, B. Kapoor, L. Alksne, K. Tabei, G. Ellestad, *Biochemistry* **2003**, *42*, 11307; c) H. Mao, S. A. Hart, A. Schink, B. A. Pollok, *J. Am. Chem. Soc.* **2004**, *126*, 2670; d) Y. Zong, T. W. Bice, H. Ton-That, O. Schneewind, S. V. L. Narayana, *J. Biol. Chem.* **2004**, *279*, 31383; e) M. W. Popp, J. M. Antos, G. M. Grotenbreg, E. Spooner, H. L. Ploegh, *Nat. Chem.*

Biol. **2007**, *3*, 707; f) M. W.-L. Popp, H. L. Ploegh, *Angew. Chem.* **2011**, *123*, 5128; *Angew. Chem. Int. Ed.* **2011**, *50*, 5024.

[9] a) M. K. M. Leung, C. E. Hagemeyer, A. P. R. Johnston, C. Gonzales, M. M. J. Kamphuis, K. Ardipradja, G. K. Such, K. Peter, F. Caruso, *Angew. Chem.* **2012**, *124*, 7244; *Angew. Chem. Int. Ed.* **2012**, *51*, 7132; b) M. P. Madej, G. Coia, C. C. Williams, J. M. Caine, L. A. Pearce, R. Attwood, N. A. Bartone, O. Dolezal, R. M. Nisbet, S. D. Nuttall, T. E. Adams, *Biotechnol. Bioeng.* **2012**, *109*, 1461; c) H. T. Ta, S. Prabhu, E. Leitner, F. Jia, D. von Elverfeldt, K. E. Jackson, T. Heidt, A. K. N. Nair, H. Pearce, C. von zur Muhlen, X. Wang, K. Peter, C. E. Hagemeyer, *Circ. Res.* **2011**, *109*, 365.

[10] a) C. von zur Muhlen, D. von Elverfeldt, J. A. Moeller, R. P. Choudhury, D. Paul, C. E. Hagemeyer, M. Olschewski, A. Becker, I. Neudorfer, N. Bassler, M. Schwarz, C. Bode, K. Peter, *Circulation* **2008**, *118*, 258; b) C. E. Hagemeyer, K. Peter, *Curr. Pharm. Des.* **2010**, *16*, 4119; c) X. Wang, C. E. Hagemeyer, J. D. Hohmann, E. Leitner, P. C. Armstrong, F. Jia, M. Olschewski, A. Needles, K. Peter, I. Ahrens, *Circulation* **2012**, *125*, 3117.

[11] a) A. Alonso, A. Della Martina, M. Stroick, M. Fatar, M. Griebe, S. Pochon, M. Schneider, M. Hennerici, E. Allemann, S. Meairs, *Stroke* **2007**, *38*, 1508; b) G. Hu, C. Liu, Y. Liao, L. Yang, R. Huang, J. Wu, J. Xie, K. Bundhoo, Y. Liu, J. Bin, *Thromb. Haemostasis* **2012**, *107*, 172.

[12] a) N. Bassler, C. Loeffler, P. Mangin, Y. Yuan, M. Schwarz, C. E. Hagemeyer, S. U. Eisenhardt, I. Ahrens, C. Bode, S. P. Jackson, K. Peter, *Arterioscler. Thromb. Vasc. Biol.* **2007**, *27*, e9; b) X. Du, E. F. Plow, A. L. Frelinger III, T. E. O'Toole, J. C. Loftus, M. H. Ginsberg, *Cell* **1991**, *65*, 409.

[13] K. Ardipradja, S. D. Yeoh, K. Alt, G. O'Keefe, A. Rigopoulos, D. W. Howells, A. M. Scott, K. Peter, U. Ackerman, C. E. Hagemeyer, *Nucl. Med. Biol.* **2014**, *41*, 229.

[14] a) T. P. Hopp, K. S. Prickett, V. L. Price, R. T. Libby, C. J. March, D. P. Cerretti, D. L. Urdal, P. J. Conlon, *Bio/Technology* **1988**, *6*, 1204; b) A. Einhauer, A. Jungbauer, *J. Biochem. Biophys. Methods* **2001**, *49*, 455.

[15] B. M. Paterson, P. Roselt, D. Denoyer, C. Cullinane, D. Binns, W. Noonan, C. M. Jeffery, R. I. Price, J. M. White, R. J. Hicks, P. S. Donnelly, *Dalton Trans.* **2014**, *43*, 1386.

[16] a) L. N. Goswami, Z. H. Houston, S. J. Sarma, S. S. Jalisatgi, M. F. Hawthorne, *Org. Biomol. Chem.* **2013**, *11*, 1116; b) K. Sano, T. Nakajima, K. Miyazaki, Y. Ohuchi, T. Ikegami, P. L. Choyke, H. Kobayashi, *Bioconjugate Chem.* **2013**, *24*, 811; c) K. A. Stephenson, R. Chandra, Z.-P. Zhuang, C. Hou, S. Oya, M.-P. Kung, H. F. Kung, *Bioconjugate Chem.* **2007**, *18*, 238.

[17] S. Pritz, Y. Wolf, O. Kraetke, J. Klose, M. Bienert, M. Beyermann, *J. Org. Chem.* **2007**, *72*, 3909.

[18] M. Schwarz, G. Meade, P. Stoll, J. Ylanne, N. Bassler, Y. C. Chen, C. E. Hagemeyer, I. Ahrens, N. Moran, D. Kenny, D. Fitzgerald, C. Bode, K. Peter, *Circ. Res.* **2006**, *99*, 25.

[19] T. Heidt, F. Deininger, K. Peter, J. Goldschmidt, A. Pethe, C. E. Hagemeyer, I. Neudorfer, A. Zirlik, W. A. Weber, C. Bode, P. T. Meyer, M. Behe, C. von zur Muehlen, *PLoS One* **2011**, *6*, e18446.

